

Androgen Receptor Targeted Conjugate for Bimodal Photodynamic Therapy of Prostate Cancer in Vitro

Valentina Rapozzi,[‡] Daniele Ragno,^{||} Andrea Guerrini,[†] Claudia Ferroni,[†] Emilia della Pietra,[‡] Daniela Cesselli,[‡] Gabriella Castoria,[§] Marzia Di Donato,[§] Emanuela Saracino,[⊥] Valentina Benfenati,[†] and Greta Varchi^{*,†}

[†]Institute of the Organic Synthesis and Photoreactivity Italian National Research Council, Via P. Gobetti, 101, 40129 Bologna, Italy

[‡]Department of Medical and Biological Sciences University of Udine, Piazzale Kolbe, 4, 33100 Udine, Italy

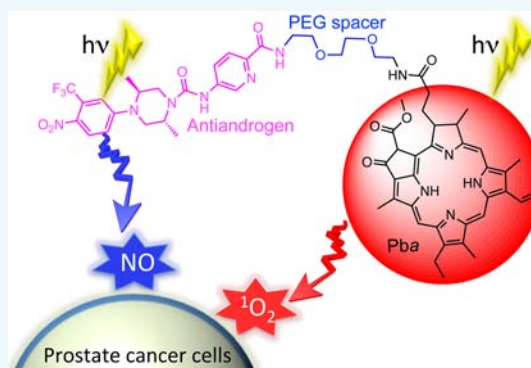
^{||}Department of Chemistry University of Ferrara, Via Fossato di Mortara, 17, 44121 Ferrara, Italy

[§]Department of Biochemistry, Biophysics and General Pathology – II University of Naples, Via L. De Crecchio, 7, 80138 Naples, Italy

[⊥]Institute for the Study of Nanostructured Materials, Italian National Research Council, Via P. Gobetti, 101, 40129 Bologna, Italy

Supporting Information

ABSTRACT: Prostate cancer (PC) represents the most common type of cancer among males and is the second leading cause of cancer death in men in Western society. Current options for PC therapy remain unsatisfactory, since they often produce uncomfortable long-term side effects, such as impotence (70%) and incontinence (5–20%) even in the first stages of the disease. Light-triggered therapies, such as photodynamic therapy, have the potential to provide important advances in the treatment of localized and partially metastasized prostate cancer. We have designed a novel molecular conjugate (**DR2**) constituted of a photosensitizer (pheophorbide *a*, Pba), connected to a nonsteroidal anti-androgen molecule through a small pegylated linker. This study aims at investigating whether **DR2** represents a valuable approach for PC treatment based on light-induced production of single oxygen and nitric oxide (NO) in vitro. Besides being able to efficiently bind the androgen receptor (AR), the 2-trifluoromethylnitrobenzene ring on the **DR2** backbone is able to release cytotoxic NO under the exclusive control of light, thus augmenting the general photodynamic effect. Although **DR2** is similarly internalized in cells expressing different levels of androgen receptor, the AR ligand prevents its efflux through the ABCG2-pump. In vitro phototoxicity experiments demonstrated the ability of **DR2** to kill cancer cells more efficiently than Pba, while no dark toxicity was observed. Overall, the presented approach is very promising for further development of AR-photosensitizer conjugates in the multimodal photodynamic treatment of prostate cancer.



INTRODUCTION

Prostate cancer (PC) is the leading cause of cancer death for men in Western countries and an emerging malignancy in developing nations.¹ Depending on the diagnosis response, PC treatment options vary. Clinicians may decide on an active surveillance or more invasive treatments such as surgical removal of the prostate gland, and external or internal radiotherapy alone or in combination with androgen depletion therapy (ADT). Despite being effective in shrinking tumor burden and improving survival, these therapies frequently fail and castration-resistant prostate cancer (CRPC) frequently develops.² At this stage, PC is almost incurable and often accompanied by metastatic spreading and poor prognosis, with a median survival range from 12 to 24 months.³ Unfortunately, few biomarkers predictive of the metastatic phenotype have been identified yet and few therapeutic options are available for CRPC patients. Although chemotherapy remains the first

choice of most clinicians at this stage, its overall benefit is very modest, since PC frequently escapes from chemotherapy at both primary and metastatic sites.^{4–6} Within the past years, several promising agents, including inhibitors of androgen synthesis or androgen receptor (AR) activation, have improved CRPC patient survival.^{7–9} Nevertheless, CRPC has evolved mechanisms to reactivate AR despite continued ADT. Therefore, further progress, beyond the discovery of more potent and selective drugs, is strongly warranted. The multimodal treatment involving the administration of different therapeutic agents acting synergistically and/or in combination with techniques has emerged as a successful approach.¹⁰ In this context, light-triggered therapies, such as photodynamic

Received: May 7, 2015

Revised: June 18, 2015

Published: June 24, 2015

therapy (PDT), have the potential to provide important advances in the treatment of localized and partially metastasized PC. PDT consists of three essential components: a photosensitizer (PS), light, and oxygen that together initiate a photochemical reaction that culminates in the generation of highly reactive oxygen species (ROS) responsible for tumor cell death.¹¹ Indeed, in June 2013 Tookad entered a randomized phase III clinical trial for vascular targeted PDT of localized PC (<https://clinicaltrials.gov/ct2/show/NCT01875393?term=NCT01875393&rank=1>). Interestingly, light can be delivered to the entire prostate gland and to nearby metastasized organs by using interstitial, cylindrically diffusing optical fibers.¹² Unlike chemotherapy or radiotherapy, the cell killing mechanism triggered by PDT is not directly dependent on DNA damage, thus decreasing the chances of therapy cross-resistance and eliminating late normal tissue effects such as second malignancy.¹³

Based on these preliminary considerations, we focused our study on the development of a novel tricomponent conjugate composed of a bacteriochlorin (pheophorbide *a*, Pba, Figure 1),¹⁴ connected to a nonsteroidal anti-androgen compound

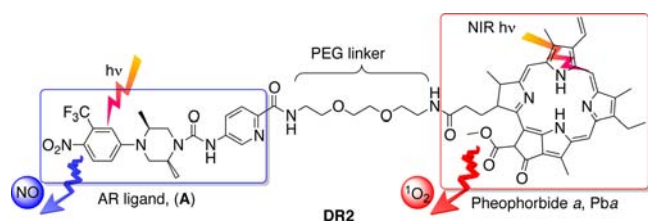


Figure 1. Chemical structure of conjugate DR2.

(Figure 1A) through a small pegylated linker, with the aim of investigating in vitro whether this compound represents a valuable approach for the targeted multimodal treatment of PC.

To this end, the synthetically modified 2,5-dimethyl-piperazine derivative A (Figure 1) was selected for (i) its high affinity to AR and ability to antagonize the receptor and (ii) the presence of the nitro substituent for the possible light-induced release of nitric oxide (NO). 2,5-Dimethyl-piperazine derivatives represent potent orally and peripherally selective nonsteroidal AR antagonists exhibiting high affinity for the AR.¹⁵ In principle, these features could favor the overall activity of the conjugate by binding to the receptor following its internalization. Recently, Dreaden and co-workers demonstrated that by binding to AR and the G-protein GPRC6A, anti-androgen-decorated gold nanoparticles exhibit enhanced therapeutic efficacy as compared to the reference drug.¹⁶ Additionally, the conjugation of an anti-androgen moiety with a histone deacetylase inhibitor (HDACi) displays higher HDACi efficacy and selectivity in PC treatment as compared to HDACi alone.¹⁷

In recent years, NO has stimulated a great deal of interest not only for its essential role in various biological functions,¹⁸ but also for its promising anticancer activity.¹⁹ NO levels in the tumor and its microenvironment can directly influence the response of cancer cells to PDT, confirming a pivotal role of exogenous NO in the overall antitumor PDT response.^{20,21} As an example, the combination of the NO donor, DETANO-NOate, and PDT resulted in significant potentiation of the cytotoxic effect in vitro and in vivo.²² Moreover, several research groups have recently developed novel NO donors to promote PDT-mediated antitumor cytotoxicity. For instance,

Carneiro and co-workers reported the synthesis and activity of a nitrosyl-phthalocyanin ruthenium complex $[\text{Ru}(\text{NO})(\text{NO})(\text{ONO})(\text{pc})]$ and studied its effect on a murine melanoma cell line, B16F10, in the presence or absence of light irradiation. Their findings demonstrated that the complex was more effective in inhibiting B16F10 cell growth than the $[\text{Ru}(\text{pc})]$, thereby confirming the importance of NO release in PDT treatment.²³

Among small molecules, the ones bearing a 2-trifluoromethylnitrobenzene ring have been established as effective NO donors as they are able to generate nitric oxide through a nitro-to-nitrite photorearrangement that occurs upon controlled irradiation with light at 400 nm wavelength (Figure 2).^{24,25}

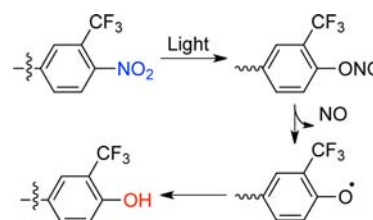


Figure 2. Light-induced NO-releasing mechanism of nitrobenzene compounds.

In this work, we present in vitro findings obtained using the newly synthesized DR2 molecular conjugate. In particular, the presented experiments focus on the ability of DR2 to be efficiently internalized in different PC cell lines and to function as a multimodal photosensitizer, thus being capable of generating ROS and NO upon light activation, thereby providing additive phototoxicity.

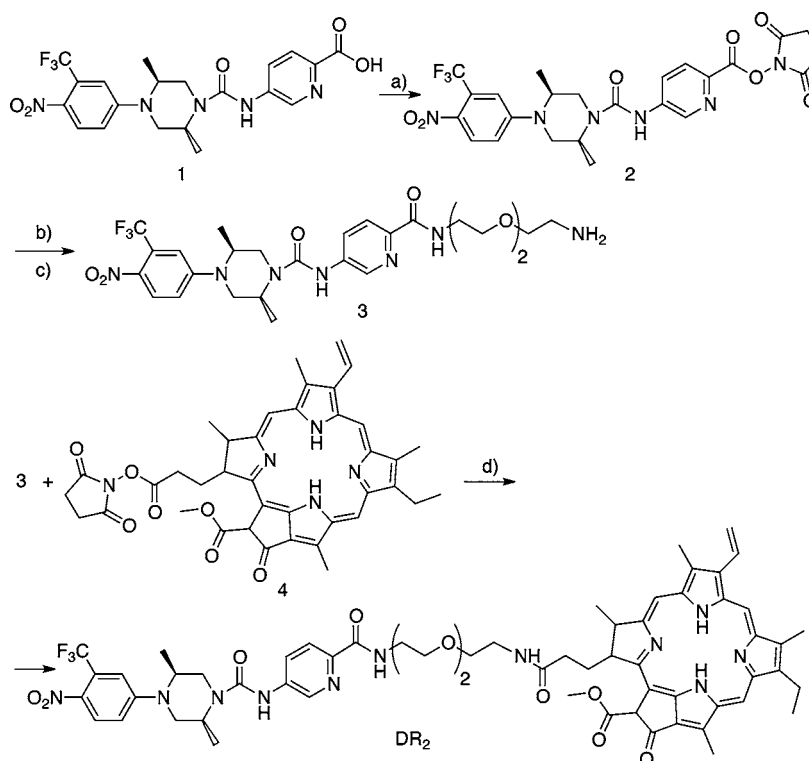
RESULTS AND DISCUSSION

Conjugate Synthesis and Characterization. Scheme 1 shows the synthesis of conjugate DR2. Acid 1 was obtained according to a slightly modified literature procedure^{15,26} (see also Supporting Information for details) and reacted with *N*-hydroxy succinimide in the presence of *N,N'*-dicyclohexylcarbodiimide (DCC) in 1,4-dioxane to afford compound 2 in good yield. Derivative 2 was then coupled with *N*-Boc-2,2'-(ethylene-1,2-dioxy)bis(ethylamine) in the presence of pyridine in tetrahydrofuran (THF), followed by deprotection of the amino group with CF_3COOH to provide compound 3 in quantitative yield. Coupling reaction between NHS-activated Pba (4) and derivative 3 was carried out in the dark and in the presence of pyridine at room temperature to provide conjugate DR2 in acceptable yield.

Whenever necessary, intermediates and final compound were purified by silica gel column chromatography and characterized by ^1H and ^{13}C NMR, and HRMS.

The electronic absorption spectra of DR2 was recorded in CH_2Cl_2 and compared with that of free Pba. The spectra of the novel conjugate show the typical features of nonaggregated Pba (Figure S1 in Supporting Information) and display a Soret band at 415 nm, slightly red-shifted with respect to Pba alone (404 nm), and an intense Q-band at 670 nm. A shoulder responsible for the absorption of the anti-androgen ligand is detected at 400 nm.

DR2 Displaces the Androgen Receptor Ligand Binding. We used the prostate cancer-derived LNCaP cells, since they represent a model to analyze the androgen-responsiveness and AR activation.²⁷ Using a siRNA approach, we first depleted

Scheme 1. Synthesis of Conjugate DR2^a

^aReaction conditions and reagents: (a) DCC, NHS, 1,4-dioxane, rt, 5 h; (45%); (b) $\text{H}_2\text{N}-[(\text{CH}_2)_2\text{O}]_2(\text{CH}_2)_2\text{NH}(\text{CO})\text{O}^t\text{Bu}$, Py, THF, rt, 21 h; (100%); (c) CF_3COOH , rt, 2 h (46%); (d) Py, THF, dark, rt, 22 h; (98%).

LNCaP cells of AR and control cells were transfected with nontargeting siRNA. Transfected cells were made quiescent and then incubated with 10 nM of the synthetic AR radioligand [^3H]-methyltrienolone ([^3H] R1881). Cells were collected and used for the ligand-binding assay. Results presented in Figure 3A show that the [^3H] R1881 binding decreases when AR was silenced. By increasing siRNA AR concentration (from 125 to 250 pmol, respectively), a parallel decrease (85% and 93%) in AR ligand binding was observed. The Western blot from lysate proteins (inset in Figure 3B), together with the densitometric analysis (Figure 3B) show that AR levels decrease as siRNA AR concentration increases. Therefore, our assay is specific for AR expressed in LNCaP cells.

The efficacy of DR2 in displacing the AR ligand binding activity was similar to that observed using unlabeled R1881, or bicalutamide, or enzalutamide, two nonsteroidal anti-androgens largely used in PC treatment,⁷ in LNCaP cells (Figure 3C). Again, a very significant [^3H] R1881 displacement was detected when the conjugate DR2 was used at 0.25 and 0.5 μM in LNCaP cells transfected with nontargeting siRNA (Figure 3D). By increasing the DR2 concentration (from 1 to 4 μM), an almost complete displacement of AR ligand binding activity was detected (Figure 3D). Similar findings were observed by using unlabeled R1881 (at 1 μM). Bicalutamide or enzalutamide shows a similar effect on AR ligand binding displacement when used at 1 μM (legend to Figure 3D). DR2 was still able to displace the [^3H] R1881 binding in LNCaP cells depleted of different amounts of AR upon siRNA AR transfection (125 and 250 pmol, respectively, in Figure 3E and F).

In sum, these findings show that DR2 specifically binds AR and is active in displacing the receptor ligand binding activity

even when low AR amounts are expressed, as it often occurs in PC-associated fibroblasts.²⁸

DR2 in Vitro Uptake and Internalization Studies in AR-Expressing PC Cells. We then evaluated the DR2 delivery/uptake in VCaP cells, which overexpress the wild type AR.²⁹ The extent of conjugate uptake over time was quantified by fluorescence-activated cell sorting (FACS). Pba displayed different behavior if administered in its free form or as DR2 conjugate. In particular, the uptake of free Pba was significant already after 3 h in VCaP [MF (mean fluorescence) = 188.89] (Figure 4A), while a longer time (6 h) was required for DR2 to reach a similar intracellular concentration [MF DR2 in VCaP = 206] (Figure 4B). Pba might passively translocate across cell membrane, while the more sterically hindered DR2 conjugate likely engages a different route to enter the cell. Furthermore, confocal microscopy analysis in Figure 4D,E demonstrates that DR2 exhibits a higher accumulation rate over time, as compared to Pba alone. This behavior might be due to its affinity for AR expressed in VCaP cells.

DR2 in Vitro Uptake and Internalization Studies in Malignant PC Cells. Prostate cancer-derived PC3 cells are highly metastatic and androgen-insensitive as they express low levels of the AR, thus representing a valuable in vitro model of castration-resistant PC.^{30,31} In order to evaluate the ability of our conjugate to be internalized by these cells, we analyzed by FACS analysis the delivery/uptake of Pba and DR2 in PC3 cells. Data in Figure 5A show that as it occurs in VCaP cells (Figure 4A), the uptake of free Pba in PC3 cells is significant already after 3 h (MF 302.88), while 6 h was required for the uptake of DR2 (MF 170). Confocal microscopy images in Figure 5D,E show that Pba and DR2 are both diffused in cytoplasm compartment after 6 h incubation. Interestingly,

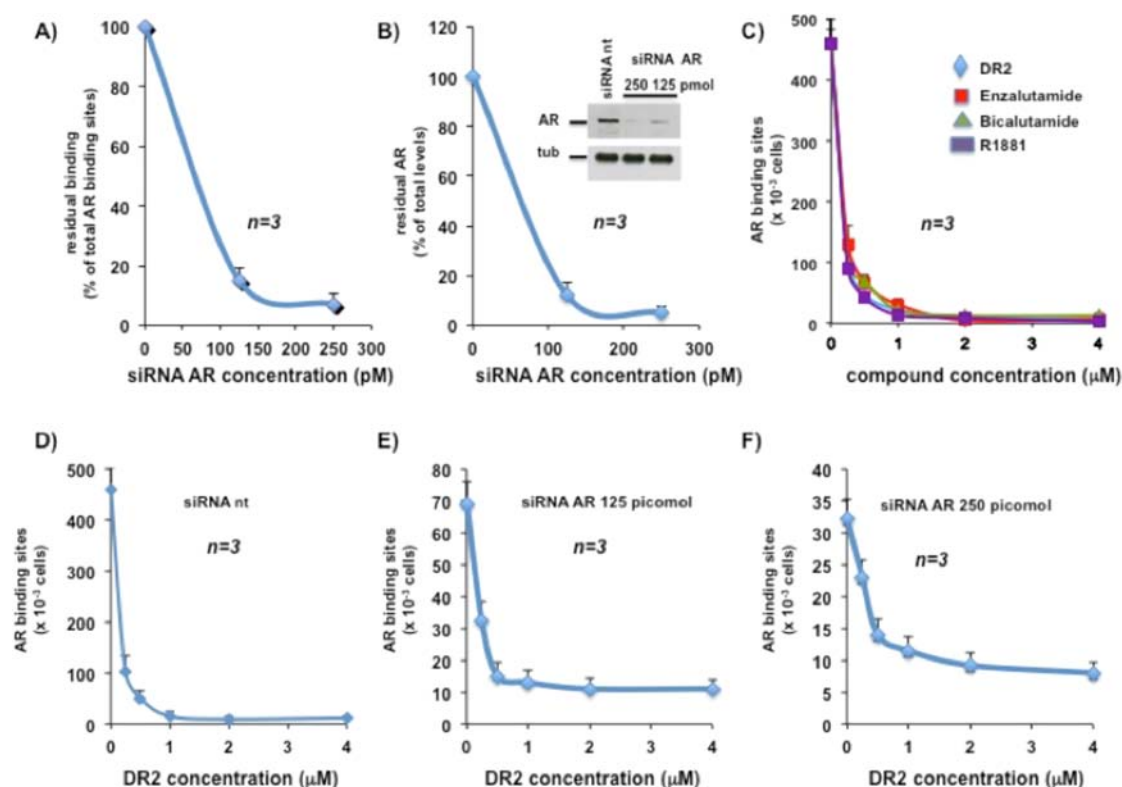


Figure 3. AR ligand binding displacement studies in LNCaP cells. (A) LNCaP cells were transfected with siRNA nt (0 on x axis) or the indicated amounts of siRNA AR. Transfected cells were incubated with 10 nM [^3H] R1881. Intracellular radioactivity was assayed and residual binding was calculated and expressed as % of total AR binding sites. Inset in B shows the Western blot of AR in the different experimental conditions. The membrane was stripped and reprobed with antitubulin antibody, as a loading control. (B) Densitometric analysis of Western blot is shown. AR levels were normalized for tubulin amounts. Residual AR was expressed as % of the total level, which corresponds to the receptor level detected in LNCaP cells transfected with siRNA nt. (C) Quiescent LNCaP cells were incubated with 10 nM [^3H] R1881, in the absence or presence of the indicated excess (from 0 to 4 μM) of DR2 or unlabeled R1881, or bicalutamide, or enzalutamide. Intracellular radioactivity was assayed and AR binding sites $\times 10^{-3}$ cells were calculated. (D–F) LNCaP cells were transfected with nt (D), or AR siRNAs (125 pM or 250 pM in (E) and (F), respectively). Cells were incubated with 10 nM [^3H] R1881, in the absence or presence of the indicated excess (from 0 to 4 μM) of DR2. Intracellular radioactivity was assayed and AR binding sites $\times 10^{-3}$ cells were calculated. In (D–F), the different values on the y axis are due to the increase in siRNA AR concentration, and hence to the parallel decrease in AR binding sites. In (A–F), data were collected from three different experiments. Means and SEM are shown.

when comparing confocal microscopy images of DR2 in VCaP and PC3 cells after 6 h of incubation, we observed that while in PC3 cells DR2 is localized exclusively in the cytoplasm, in VCaP cells red fluorescence is intensively diffused also in the nucleus (cf., Figures 4E and 5E). This result might suggest that DR2 translocates into the nucleus upon binding to the receptor, as also confirmed by the binding experiment performed with the radioligand assay (Figure 3). However, more studies are underway to verify the role of DR2 after the binding to the androgen receptor in terms of gene transcription activity.

Despite the fact that DR2 internalization seems to be slightly slower in PC3 cells as compared to VCaP cells (cf., Figures 4C and 5C), DR2 is persistently present after 24 h of incubation in PC3 cells (MF 422). In contrast, the amount of Pba is significantly reduced (MF 249) at that incubation time (Figure 5C), likely because of its efflux. This behavior draws our attention to the emerging problem of PDT resistance,³² and in particular to Pba as substrate for the ABCG2 pump efflux.^{33–35} The ABCG2 gene encodes a membrane transporter belonging to the ATP-binding cassette (ABC) superfamily of membrane transporters, which being involved in the trafficking of a variety of biological molecules and drugs across the plasma membrane,

also plays a role in multidrug resistance. To investigate more deeply this aspect and the possible beneficial role of conjugating the photosensitizer with specific targeting antenna, we performed an experiment with A549 human lung adenocarcinoma cells that express higher levels of ABCG2, as compared with PC3 cells (Figure 6A,B).

Robey and co-workers described a functional assay to evaluate if different photosensitizers are substrates for this efflux pump, using an ABCG2 inhibitor, e.g., reserpine.^{34,36,37} Therefore, in order to determine whether DR2 is a substrate for ABCG2 pump, we incubated A459 cells with 5 μM of Pba or DR2 in the presence or absence 10 μM of reserpine for 30 min. Subsequently, the cells were washed and incubated for 1 h in a photosensitizer-free medium in the presence of reserpine. Graphs in Figure 6C report the fluorescence of Pba (left) and DR2 (right), alone (blue lines) or plus reserpine (red lines), respectively. Reserpine increases the accumulation of Pba in the PC3 cells, while no shift of the fluorescence peak is observed by using DR2, thus suggesting that DR2 is not a substrate for the efflux pump.

In sum, data in Figures 4, 5, and 6 show that DR2 conjugate binds with high affinity AR and escapes the ABCG2 efflux pump in PC3 cells. These properties make DR2 a promising

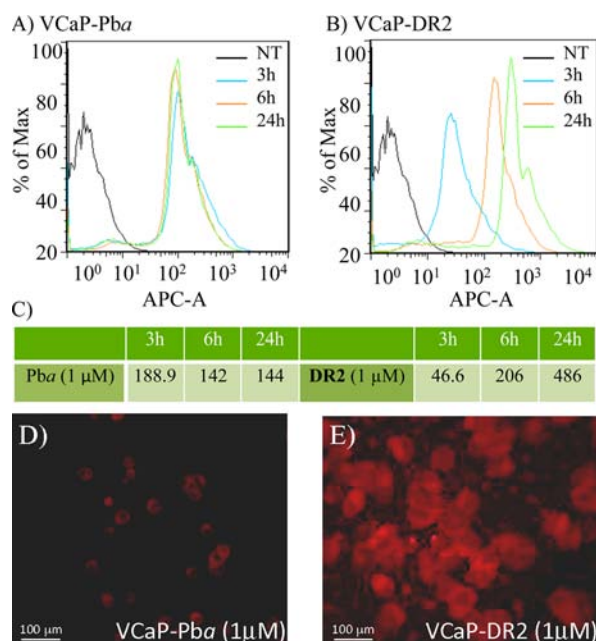


Figure 4. Uptake of Pba and DR2 on VCaP cells. (A,B) FACS analyses of VCaP cells treated with 1 μM of Pba and DR2. (C) Values of mean of fluorescence (MF) at different time of photosensitizer incubation. Fluorescence was detected after 3, 6, and 24 h from compound incubation. Data were collected from three different experiments. (D,E) High magnification (40×) single plane confocal images representative of fluorescence emission collected by VCaP cells after 6 h of incubation with 1 μM Pba (D) and 1 μM DR2 (E). Bar is 100 μm.

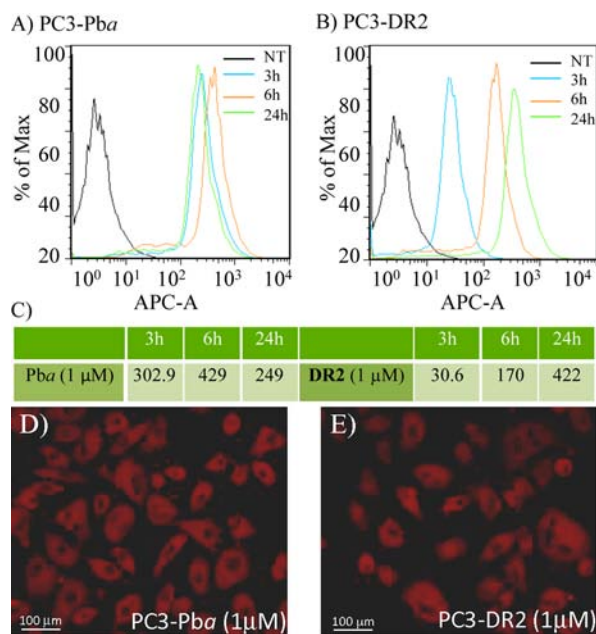


Figure 5. Uptake of Pba and DR2 on PC3 cells. (A–C) FACS analyses of PC3 cells treated with 1 μM of Pba and DR2. (C) Values of mean of fluorescence after different time of photosensitizer incubation. Fluorescence was detected after 3, 6, and 24 h from compound incubation. Data were collected from three independent experiments (D,E). High magnification (40×) single plane confocal images representative of fluorescence emission collected by PC3 cells after 6 h of incubation with 1 μM Pba (D) and 1 μM DR2 (E). Bar is 100 μm.

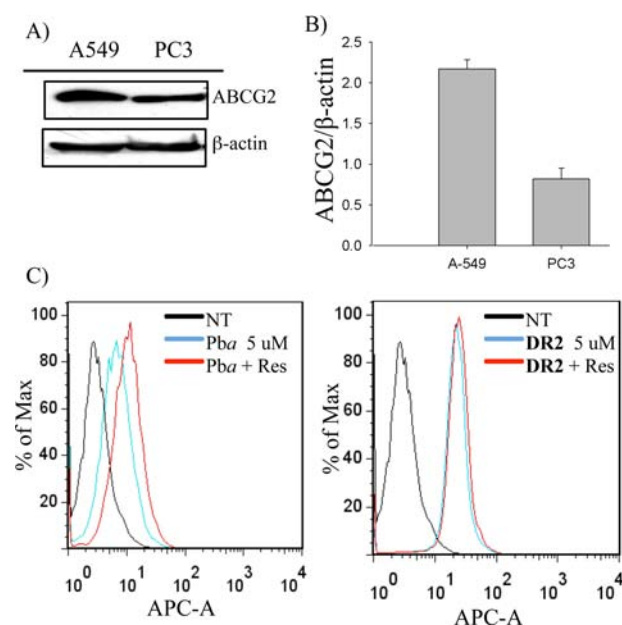


Figure 6. (A) Western blot of ABCG2 and β-actin protein levels in A549 and PC3 cell lines. (B) Histograms report the values of the ABCG2 protein band intensity determined by densitometric analysis and normalized for β-actin. (C) Functional assay for ABCG2 substrate. The A549 cells were incubated with 5 μM of Pba or DR2 for 30 min with or without 10 μM reserpine, washed, and then incubated for 60 min in PS-free media with a red line) or without (blue line) reserpine. Intracellular fluorescence was determined using a flow cytometer equipped with a 633 nm red diode laser. Representative results from two independent experiments are shown.

candidate for PDT in PC, since it is retained in PC cells expressing different levels of AR. In this latter setting, DR2 consistently accumulates within PC cells, preventing the onset of PDT resistance.³²

In Vitro Photodynamic Activity. The in vitro photodynamic activity of DR2 was investigated against LNCaP, VCaP, and PC3 cells. Twenty-four hours after light irradiation, cell proliferation was determined by resazurin assay using free Pba as reference. Pba presents a Q-band absorption peak at 670 nm allowing irradiation with a red light, while the *o*-CF₃ nitrobenzene group (AR ligand moiety) should release NO upon selective irradiation at 400 nm. Therefore, in order to stimulate both compounds, cells were initially irradiated with a white halogen light covering the entire visible spectrum.

According to the results of the uptake experiments, cells were incubated in the dark with increasing concentrations of Pba and DR2 for 6 h and subsequently irradiated with a metal white halogen lamp for 30 min (7 J/cm²). Data shown in Figure 7A–C account for a higher phototoxicity of DR2 in all cell lines as compared to Pba alone. Remarkably, the IC₅₀ values (defined as the compound concentration to inhibit 50% of the cells) of DR2 were lower than Pba in all cell lines (Table 1), when using white light. This might be due to the longer retention of DR2 inside the cells and to the ability of the NO-donor moiety to induce the release of NO species that are synergistic to ¹O₂ generated by Pba. Importantly, no dark toxicity was observed for the conjugate 24 h after treatment (Figure S2).

In order to evaluate the contribution of NO to the overall toxicity of the new conjugate, we performed a second set of metabolic assays using a halogen lamp equipped with a red filter, with the aim to excite only Pba. Results on PC3, LNCaP,

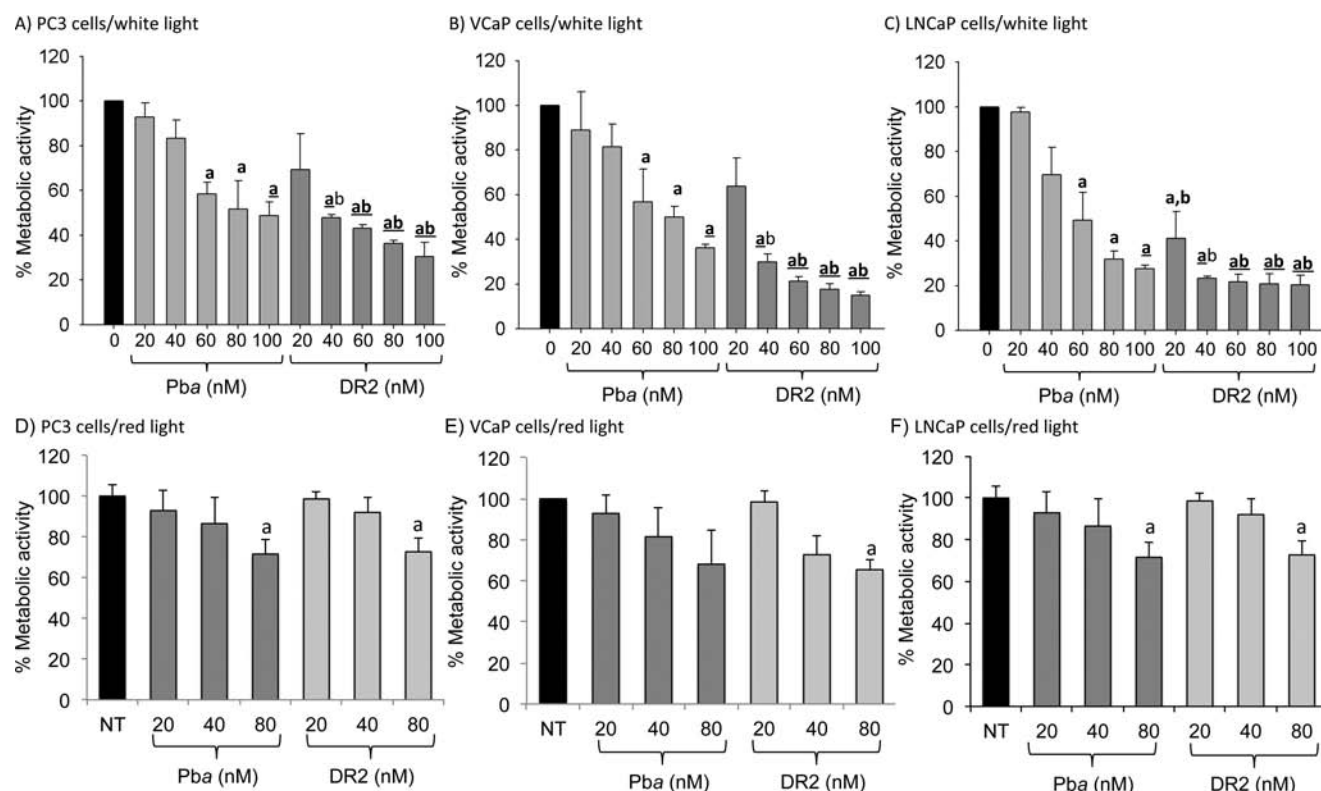


Figure 7. Metabolic activity (%) of PC3, VCaP, and LNCaP cells treated with increasing amounts of Pba and DR2. After 6 h incubation in the dark the cells were irradiated (A–C) with a white halogen lamp (fluence 7.2 J/cm²) and (D–F) with the same lamp equipped with a red filter (fluence 0.84 J/cm²). A resazurin assay was carried out 24 h after irradiation. Data represent mean values \pm SD of three independent experiments. T-Test analysis of different treatments (Pba and DR2) vs NT: a, $p < 0.05$; **a**, $p < 0.01$; DR2 vs Pba: b, $p < 0.05$; **b**, $p < 0.01$.

Table 1. IC₅₀ Values of Pba and DR2 upon White and Red Light Irradiation on a Panel of Prostate Cancer Cell Lines^a

| compound | IC ₅₀ [nM] | | | | | |
|----------|-----------------------|--------------|----------------------|------------|--------------------|------------|
| | VCaP ^{b,c} | | LNCaP ^{b,c} | | PC3 ^{b,c} | |
| | white light | red light | white light | red light | white light | red light |
| Pba | 78.9 \pm 0.96 | 94 \pm 3.2 | 60.1 \pm 2.1 | 65 \pm 5 | 82.1 \pm 1.9 | 95 \pm 6 |
| DR2 | 25.3 \pm 1.10 | 96 \pm 5.0 | 12.0 \pm 1.4 | 70 \pm 6 | 35.1 \pm 2.8 | 98 \pm 5 |

^aSix hours after incubation in the dark with the compounds, cells were irradiated with a metal white halogen lamp (alone or equipped with a red filter) for 30 min. ^bThe reported values are the IC₅₀ expressed in nanomolar. ^c $P < 0.05$ (t test) DR2 vs Pba. Data represent mean values \pm SD of three independent experiments.

and VCaP cells are reported in Figure 7D–F and Table 1, confirming that no difference occurs in the phototoxic behavior of the two compounds when irradiated with red light, thereby supporting the additive action of the NO released only when white lamp is used as light source.

In parallel, a Griess test was performed to evaluate the nitrite production. After 24 h incubation at 37 °C, the cells were treated with different concentrations of Pba and DR2 and irradiated with white or red light. After 1 h from irradiation the cell supernatants were collected and NO production was evaluated by addition of the Griess reagent. Nitrite concentration was determined by measuring the absorbance at 540 nm with respect to a standard curve of NaNO₂ diluted in culture medium.

Data reported in Figure 8 successfully account for a higher nitrite production by DR2, as compared to Pba under white light irradiation. This effect is particularly evident in VCaP cells (Figure 8A). The extent of NO₂ production induced by red light is almost negligible (Figure 8B), thus confirming the

effective production of NO radicals induced by the AR ligand present on the DR2 backbone.

In conclusion, the reported data indicate that DR2 is a novel and promising photosensitizer for the multimodal treatment of prostate cancer. Cell death increase is observed in all considered cell lines. This effect is likely associated with the synergistic/additive action of the ROS generated by the photosensitizer moiety (Pba) and the NO released upon irradiation of the AR ligand moiety with white light. Moreover, DR2 exhibits a constant and time-dependent fluorescence increase even after 24 h of incubation in both VCaP and PC3 cells. This behavior might be due to the concomitant affinity of the conjugate for the AR that might favor its internalization and accumulation in tumor cells, and to the ability of DR2 to escape the ABCG2 efflux pump mechanism which is responsible for Pba excretion from the cells. This result is particularly important if considering that PC3 cells lack the AR and are representative of an advanced stage of the disease.

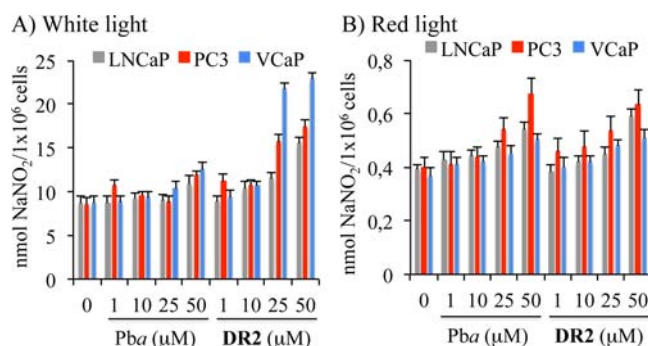


Figure 8. Nitric oxide detection by Griess test. Effects of different amounts (0–50 μM) of Pba and DR2 on nitric oxide production in PC cells after (A) white light irradiation and (B) red light irradiation. Nitrite concentrations were determined by comparing the absorbance values for the test samples to a standard curve generated by serial dilution of 100 mmol/L sodium nitrite. Results of NO production are expressed as nmol $\text{NO}_2^-/10^6$ cells and are collected from two different experiments.

DR2 displays very promising features of selectivity and controlled phototoxicity in a variety of PC cell lines, while being totally nontoxic in the dark. Overall, these characteristics make DR2 a promising candidate for further investigations in PC in vivo models.

EXPERIMENTAL PROCEDURES

Materials Chemistry. All solvents and reagents were used as obtained from commercial sources unless otherwise indicated. Solvents and reagents were obtained from Sigma-Aldrich (Schnelldorf, DE). Pba was purchased from Frontier Scientific (Catalog # Pha-592) and used without further purification.

Materials Biology. Unlabeled R1881, bicalutamide, reserpine, PBS-0.01% Tween, Griess reagent [1% sulfanilamine in 30% acetic acid with 0.1% *N*-(naphthyl)ethylenediamine dihydrochloride in 60% acetic acid] and resazurin assay were obtained from Sigma-Aldrich, Milan, Italy and enzalutamide from Selleckchem. PC3 and VCaP cells were purchased from Experimental Zooprophyllactic Institute of Lombardia and Emilia Romagna. Prostate cancer-derived fast-growing LNCaP cells were from ATCC (U.S.A.). A549 cells were obtained by Professor G. Tell (Department of Medical and Biological Sciences, University of Udine, Italy). Dulbecco's Modified Eagle Media (DMEM), Fetal Bovine Serum (FBS), Insulin, antibiotics (Penicillin/Streptomycin), RPMI1640, and Pen/Strepto were purchased from Gibco. Nontargeting siRNAs, containing a scrambled sequence, rabbit polyclonal anti-AR (N-20) or anti-ABCG2 (B-25:sc-130933) antibodies were purchased from Santa-Cruz Biotechnologies. Mouse monoclonal anti-tubulin antibody was from Sigma-Aldrich. Lipofectamine 2000 was from Invitrogen. [^3H]-R1881 (98 Ci/mmol) was purchased by PerkinElmer. Mouse monoclonal anti- β -actin (Ab-1, CP01), anti-rabbit IgG, and anti-mouse IgM were obtained from Calbiochem. Super SignalWest PICO and Super SignalWest FEMTO were from ThermoFisher Scientific Pierce, Rockford, USA.

Methods Chemistry. All reactions were performed under nitrogen atmosphere unless otherwise noted. Flash chromatography was performed on Teledyne Isco CombiFlash Rf 200 using RediSep Normal-phase Silica Flash Columns (230–400 mesh). The reactions were monitored by TLC using silica gel

60 F254 with detection by charring with KMnO_4 . UV spectra were registered with a Lambda 20 PerkinElmer spectrophotometer. NMR spectra were recorded in CDCl_3 , $(\text{CD}_3)_2\text{CO}$, or CD_3OD solutions at 25 $^\circ\text{C}$ on a Varian Mercury spectrometer operating at 400 MHz (^1H) and 100.5 MHz (^{13}C). When present, the water signal in the ^1H NMR spectra was suppressed using postelaboration solvent suppression sequence.

^1H Chemical shifts values (δ) are referenced to the residual nondeuterated components of the NMR solvents ($\delta = 7.26$ ppm for CHCl_3 and $\delta = 3.31$ ppm for CHD_2OD , etc.). The ^{13}C chemical shifts (δ) are referenced to CDCl_3 (central peak, $\delta = 77.0$ ppm), CD_3OD ($\delta = 49.0$ ppm), etc. as the internal standard. The IR spectra were registered with a PerkinElmer Spectrum BX FT-IR System. For accurate mass measurements, the compounds were analyzed in positive ion mode by Agilent 6520 HPLC-Chip Q/TOF-MS (nanospray) using a quadrupole, a hexapole, and a time-of-flight unit to produce the spectra. The capillary source voltage was set to 1700 V; the gas temperature and drying gas were kept at 350 $^\circ\text{C}$ and 5 L min^{-1} , respectively. The MS analyzer was calibrated externally with the ESI-L low concentration tuning mix from m/z 118 to 2700 to yield an accuracy below 5 ppm. Accurate mass data was collected by directly infusing samples in 40/60 $\text{H}_2\text{O}/\text{ACN}$ 0.1% TFA into the system at a flow-rate of 0.4 $\mu\text{L min}^{-1}$. FEP tubing, 1/16" ϕ - 1.0 mm ID and PTFE tubing, 1/16" ϕ - 1.0 mm ID were purchased from VICI Jour.

Chemistry. Acid 1. Methyl ester (S2) (1 equiv) was than dissolved in methanol (10 mL/mmol) and a few drops of THF. NaOH (1 N) (1 equiv) was then added to the solution, which was stirred for 24 h at room temperature. A white precipitate formed that was filtered off and dried under vacuum affording acid (1) as pure compound in 80%. ^1H NMR (400 MHz, CD_3OD) δ 9.03 (bs, 1H), 8.37 (d, $J = 8.7$ Hz, 1H), 8.26 (d, $J = 8.2$ Hz, 1H), 8.04 (d, $J = 8.9$ Hz, 1H), 7.26 (d, $J = 1.9$ Hz, 1H), 7.19 (d, $J = 9.1$ Hz, 1H), 4.62 (bs, 1H), 4.39 (bs, 1H), 4.01 (d, $J = 13.5$ Hz, 1H), 3.73–3.54 (m, 2H), 3.55 (d, $J = 12.0$ Hz, 1H), 1.34 (d, $J = 6.0$ Hz, 3H, CH_3), 1.25 (d, $J = 6.4$ Hz, 3H, CH_3). ^{13}C NMR (100 MHz, CD_3OD) δ 171.84, 155.26, 153.35, 142.27, 137.69, 137.01, 136.74, 130.48, 128.64, 126.58, 124.14, 121.43, 115.25, 111.70, 60.38, 49.72, 45.29, 43.12, 14.98, 12.25. HRMS (m/z) calcd for $\text{C}_{20}\text{H}_{20}\text{F}_3\text{N}_5\text{O}_5$ [M] $^+$, 468.1417; found, 468.1420.

Activated Acid 2. *N*-Hydroxysuccinimide (1 equiv) and DCC (1 equiv) were subsequently added to a solution of the acid (1) (1 equiv) in 1,4-dioxane (14 mL/mmol of 1). The reaction mixture was stirred at room temperature for 5 h and then diluted with THF. The obtained solution was absorbed on SiO_2 and evaporated under vacuum. The resulting solid was purified by silica gel flash chromatography ($\text{CH}_2\text{Cl}_2/\text{Et}_2\text{OAc}/\text{cHex} = 1/2/2$) affording the desired compound in 70% yield. ^1H NMR (400 MHz, CD_3OD) δ 8.87 (bs, 1H), 8.24–8.12 (m, 2H), 8.04 (d, $J = 9.2$ Hz, 1H), 7.26 (d, $J = 2.3$ Hz, 1H), 7.18 (dd, $J_1 = 9.4$, $J_2 = 2.8$ Hz, 1H), 4.62–4.56 (m, 1H), 4.40–4.32 (m, 1H), 4.25–4.17 (m, 1H), 3.99–3.91 (m, 1H), 3.73–3.65 (m, 2H), 2.91 (s, 4H, 2 CH_2), 1.33 (d, $J = 6.7$ Hz, 3H, CH_3), 1.23 (d, $J = 6.6$ Hz, 3H, CH_3). ^{13}C NMR (100 MHz, CD_3OD) δ 171.70, 156.67, 154.52, 143.50, 142.58, 137.38, 136.74, 130.48, 128.64, 126.58, 124.14, 116.34, 112.78, 49.72, 48.47, 48.04, 45.29, 43.12, 26.7, 16.10, 13.46. HRMS (m/z) calcd for $\text{C}_{24}\text{H}_{23}\text{F}_3\text{N}_6\text{O}_7$ [M] $^+$, 565.1580; found, 565.1585.

Compound 3. To a solution of *tert*-butyl (2-(2-(2-aminoethoxy)ethoxy)ethyl)carbamate³² (1 equiv) in dry THF (3.2 mL/mmol), pyridine (1.4 mL/mmol) was added dropwise

followed by succinimidyl derivative (**2**) (1 equiv). The reaction mixture was then stirred at room temperature for 24 h (complete disappearance of the starting material). The mixture was then diluted with EtOAc and the organic layer was washed several times with distilled water. The collected organic phase was then dried over Na_2SO_4 , filtered, and evaporated under reduced pressure. The crude material was successively treated with CF_3COOH (28 mL/mmol of starting acid) and stirred at room temperature for 3 h. The reaction mixture was subsequently diluted with distilled water and basified (pH = 10) with NaHCO_3 . The organic phase was then extracted with EtOAc and dried over anhydrous Na_2SO_4 , filtered, and concentrated under reduced pressure to afford (**3**) as pure compound in 70% yield. ^1H NMR (400 MHz, CD_3OD) δ 8.73 (bs, 1H), 8.05 (d, J = 9.6 Hz, 3H), 7.27 (d, J = 2.8 Hz, 1H), 7.21–7.11 (m, 1H), 4.63–4.57 (m, 1H), 4.41–4.32 (m, 1H), 4.02–3.92 (m, 2H), 3.69–3.54 (m, 6H), 3.55–3.39 (m, 2H), 2.94–2.75 (m, 1H), 1.33 (d, J = 6.6 Hz, 3H, CH_3), 1.24 (d, J = 6.7 Hz, 3H, CH_3). ^{13}C NMR (101 MHz, CD_3OD) δ 165.54, 156.08, 153.38, 150.16, 143.58, 140.53, 134.29, 132.05, 131.32, 128.60, 127.39, 122.09, 115.21, 75.95, 70.18, 70.15, 69.46, 51.80, 49.78, 45.33, 43.06, 40.10, 39.05, 25.57, 24.88, 14.93, 12.27. HRMS (m/z) calcd for $\text{C}_{26}\text{H}_{33}\text{F}_3\text{N}_6\text{O}_7$ [M] $^+$, 599.2363; found, 599.2370.

Conjugate DR2. Compounds (**4**) (see Supporting Information for detailed synthesis) (1 equiv) and (**3**) (1.2 equiv) were placed in a two-necked round bottomed flask under nitrogen and in the dark. Then, THF (40 mL/mmol) was added followed by pyridine dropwise (16 mL/mmol). The reaction mixture was stirred at room temperature for 24 h, monitoring the disappearance of the starting material by TLC. The reaction mixture was then diluted with EtOAc and washed several times with distilled water. The collected organic phases were then dried over Na_2SO_4 , filtered, and concentrated under reduced pressure. The crude material was then purified by silica gel flash column chromatography ($\text{CH}_2\text{Cl}_2/\text{MeOH}$ = 14/1) affording **DR2** in 98% yield.

^1H NMR (400 MHz, CDCl_3) δ 9.41 (d, J = 11.7 Hz, 1H), 9.31 (d, J = 6.4 Hz, 1H), 8.61 (bs, 1H), 8.51 (bs, 1H), 8.42 (bs, 1H), 8.19–8.15 (m, 1H), 8.11–7.90 (m, 3H), 7.68 (dd, J_1 = 10.4 Hz; J_2 = 3.0 Hz, 1H), 7.29 (dd, J_1 = 7.6 Hz; J_2 = 5.0 Hz, 1H), 6.32–6.16 (m, 3H), 4.49–4.37 (m, 2H), 4.23–4.15 (m, 3H), 3.87 (d, J = 9.0 Hz, 3H), 3.75–3.61 (m, 7H), 3.52–3.39 (m, 7H), 3.36 (d, J = 3.6 Hz, 6H), 3.20 (d, J = 5.2 Hz, 6H), 2.50–2.38 (m, 4H), 1.83 (d, J = 7.6 Hz, 3H), 1.75 (d, J = 7.3 Hz, 3H), 1.33 (d, J = 6.8 Hz, 3H), 1.23 (d, J = 6.8 Hz, 3H). ^{13}C NMR (101 MHz, CDCl_3) δ 189.80, 173.12, 172.44, 170.32, 164.51, 157.09, 154.88, 152.71, 149.98, 145.66, 144.05, 142.59, 139.70, 139.19, 138.03, 137.06, 136.68, 132.45, 129.04, 127.52, 126.66, 126.26, 123.84, 123.38, 122.77, 121.12, 114.39, 111.84, 104.68, 93.77, 93.56, 70.13, 69.79, 65.18, 53.37, 51.61, 50.55, 49.34, 46.84, 45.56, 43.20, 39.13, 34.16, 33.38, 30.56, 29.92, 25.81, 25.16, 23.33, 19.62, 17.54, 16.06, 13.10, 12.30, 11.43. HRMS (m/z) calcd for $\text{C}_{61}\text{H}_{68}\text{F}_3\text{N}_{11}\text{O}_{10}$ [iM] $^+$, 1172.5103; found, 1172.5109.

Cell Culture Experiments. *Cell Culture.* PC3 and LNCaP cells were cultured in RPMI 1640 medium, while VCaP and A549 cells in DMEM. Both media contained 10% FBS, antibiotics (penicillin 100 U/mL, streptomycin 100 $\mu\text{g}/\text{mL}$) and glutamine 2 mM. Cells were maintained in a humidified atmosphere with 5% CO_2 air at 37 $^\circ\text{C}$. Unless otherwise stated, experiments were performed using cells at the exponential growth phase.

siRNA AR Experiments and AR Ligand Binding Displacement Studies. For AR binding experiment LNCaP cells were cultured in RPMI 1640 supplemented with 10% fetal calf serum and made quiescent as reported.²⁷ After reaching subconfluence, growing LNCaP cells were used for AR siRNA experiments, using a pool of 4 target-specific 20–25 non-targeting or AR siRNAs, as reported.³⁸ siRNAs were transfected using LipofectamineTM 2000. After transfection, the cells were kept in phenol red-free RPMI 1640 medium containing 5% charcoal-stripped calf serum and Pen/Strepto for 24 h. Transfected cells were then used for ligand binding studies or WB analysis. For AR ligand binding studies, untransfected or transfected LNCaP cells were incubated at 37 $^\circ\text{C}$ for 4 h with 10 nM of [^3H] R1881 to the medium, in the absence or presence of the indicated excess of radio-inert compounds (R1881, bicalutamide, enzalutamide, or DR2), as previously described.³⁹ Cells were then washed three times with ice-cold PBS and collected by gently scraping in the cold room using 600 μL of ice-cold PBS containing 0.05% EDTA (w/v). The number of cells in an aliquot of 100 μL was counted. Aliquots (400 μL) of cell suspension were used in duplicate to extract the intracellular radioactivity in 1000 μL ice-cold ethanol (100%) for 2 h. After 24 h at 37 $^\circ\text{C}$, the radioactivity was counted in a liquid scintillation counter. Nonspecific binding of [^3H]-R1881 was always determined in separate wells by adding 1 μM of unlabeled R1881 to the incubation medium, as a control. The Western blot analysis was done using cell lysates (at 2 mg/mL protein concentration) as described.²⁴ AR was detected using the rabbit polyclonal anti-AR antibodies (N-20; Santa Cruz). The mouse monoclonal anti-tubulin antibody (Sigma) was used to detect tubulin. Immune-reactive proteins were revealed using the ECL detection system (GE Healthcare).

Fluorimetric Determination of Cellular Uptake. VCaP, LNCaP, and PC3 cells were seeded in a 6-well plate at a cell density of 6×10^5 cells/well. The day after, the cells were treated with Pba and **DR2** at concentration of 1 μM . At different times of incubation in the dark (3–6–24 h), the cells were harvested, washed twice, resuspended in 0.5 mL of PBS, and analyzed by a FACSARIA 3 (Becton Dickinson, San Jose, USA) equipped with a 633 nm laser. A minimum of 10 000 cells per sample was acquired in list mode and analyzed using FLOWJO software. The signal was detected by APC-A in log scale.

Confocal Microscopy Studies. VCaP and PC3 were seeded on 19 mm coverslips coated with FBS, evaporated overnight, and placed into 12 multiwell plate at the concentration of 5×10^3 per sample, thus allowing the best cell confluence at 24 h and imaging experiments. Pba and **DR2** [1 μM] were then added to the cell medium from a stock solution (1 mL) and samples were kept in the incubator covered from the light. After 4 h of incubation, all the samples were washed three times for 1 min with PBS before performing confocal experiments. Optical imaging was performed with a Nikon TE 2000 inverted confocal microscope equipped with 40 \times objective and Hamamatsu CCD camera. Coverslips were then mounted by means of a custom-made chamber onto Nikon TE2000 inverted microscope and fluorescence images were collected at 543 nm He Ne laser as excitation source. Images reported are representative of 2 different experiments, performed in triplicate.

Expression of ABCG2 by Western Blotting. For this experiment we have compared the protein level of ABCG2 in

A549 lung carcinoma cells and in PC3 cells. The extracted proteins (40 μ g) were subjected to electrophoresis on 12% SDS–PAGE and transferred to a nitrocellulose membrane 70 V for 2 h. The filter was blocked for 1 h with PBS–0.01% Tween containing 5% dry nonfat milk, and then incubated, at 4 °C overnight, with the primary antibody, rabbit polyclonal ABCG2 diluted 1:100. The expression of β -actin, used as an internal control, was detected with a mouse monoclonal anti- β -actin (Ab-1, CP01) diluted 1:10 000. The filters were incubated for 1 h with the secondary antibodies with either anti-rabbit IgG diluted 1:4000 or anti-mouse IgM, diluted 1:5000. Each secondary antibody was coupled to horseradish peroxidase (HPR). For the detection of the proteins, we used ECL (enhanced chemiluminescence) reagents (Super SignalWest PICO, and Super SignalWest FEMTO). The exposure length depended on the antibodies used and was usually between 30 s and 5 min. The protein levels were quantified by Image Quant TL v 2003 software (Amersham).

Flow Cytometry Pba and DR2 Uptakes after ABCG2 Inhibitor Treatment. A549 cells were seeded at the density of 6×10^5 cells/well. The day after, cells were incubated (30 min in the dark) in complete medium with the desired photosensitizer (5 μ M Pba or DR2) with or without 10 μ M of ABCG2 inhibitor, reserpine (Sigma-Aldrich, Milan, Italy), an ABCG2 inhibitor. After this time, the cells were incubated in photosensitizer-free fresh medium, with or without 10 μ M reserpine for 1 h. The cells were harvested, washed twice, and resuspended in PBS. The photosensitizer uptake was measured by FACSARIA 3 (Becton Dickinson, San Jose, USA) equipped with a 633 nm laser. A minimum of 10 000 cells for sample was acquired in list mode and analyzed using FLOWJO software. The signal was detected by APC-A in log scale.

Photodynamic Treatment. Pba and DR2 were dissolved in dimethyl sulfoxide (DMSO) and conserved in aliquots of 0.5 mM at -80 °C. Their stability in solution was checked by measuring their UV–vis spectrum at weekly intervals. Cells were incubated with different concentration of the compounds in the dark and then irradiated with a metal white halogen lamp for 30 min (7 J/cm²) or with red filter for 7 min (0.84 J/cm²) depending on the experimental conditions. Fluency for red light was assessed on the basis of the IC₅₀ of Pba with white light.

Cell Metabolic Assay. PC cells were seeded in a 96-well plate at a density of 5×10^3 cells/well. The following day, Pba and DR2 were added at different concentrations and incubated for 6 h in the dark and then light irradiated. Twenty-four hours after irradiation, the metabolic activity was determined by the resazurin assay following the manufacturer's instructions (Sigma–Aldrich, Milan, Italy). The fluorescence was measured with a spectrofluorimeter (EnSpire™ 2300 Multilabel reader, PerkinElmer, Finland). The data are presented as the percentage of metabolic activity compared to that of untreated cells. The data are the average of at least three independent experiments. The protocol for PDT is reported in the figure captions.

Nitric Oxide Detection by Griess Test. PC cells were seeded in a 96-well plate at a density of 10^4 cells/well. After 24 h incubation at 37 °C, the cells were treated with different concentrations of Pba and DR2 in DMEM without phenol red. After 24 h, cells were irradiated with white or red light and after 1 h equal volumes of culture supernatants were collected and mixed. Cell supernatants were collected and mixed with Griess reagent (Sigma-Aldrich). After incubation at room temperature for 15 min, the absorbance was measured at 540 nm with

EL808 Ultra Microplate Reader (BIO-TEK Instruments, Inc., Vermont USA). Nitrite concentrations were determined by comparing the absorbance values for the test samples to a standard curve generated by serial dilution of 100 mmol/L sodium nitrite. Results of NO production are expressed as nmol NO₂[−]/10⁶ cells.

■ ASSOCIATED CONTENT

● Supporting Information

Experimental procedures, spectroscopic data, and copies of ¹H/¹³C NMR of new compounds; additional figures and tables on biological experiments. The Supporting Information is available free of charge on the ACS Publications website at DOI: 10.1021/acs.bioconjchem.5b00261.

■ AUTHOR INFORMATION

Corresponding Author

*E-mail: greta.varchi@isof.cnr.it. Phone: +39 0516398283. Fax +39 0516398349.

Notes

The authors declare no competing financial interest.

■ ACKNOWLEDGMENTS

The work done by Prof. Gabriella Castoria and Dr. Marzia Di Donato was supported by grants from the Italian Ministry of University and Scientific Research (P.R.I.N. 2010NFEB9L_002). M.D.D is a recipient fellowship of a PRIN Grant (2010NFEB9L_002).

■ DEDICATION

In memory of Professor Giulio Jori.

■ ABBREVIATIONS

ABC, ATP-binding cassette; ABCG2, ATP-binding cassette subfamily G member 2; ADP, androgen receptor therapy; AR, androgen receptor; CF₃, trifluoromethyl; CRPC, castration-resistant prostate cancer; DCC, *N,N'*-dicyclohexylcarbodiimide; GPRC6A, G protein-coupled receptor, class C, group 6, member A; HRMS, high resolution mass spectroscopy; MF, mean of fluorescence; NMR, nuclear magnetic resonance; NO, nitric oxide; PC, prostate cancer; PDT, photodynamic therapy; PS, photosensitizer; ROS, reactive oxygen species; siRNA, small interference RNA; THF, tetrahydrofuran

■ REFERENCES

- (1) Jemal, A., Siegel, R., Ward, E., Hao, Y., Xu, J., and Thun, M. J. (2009) Cancer statistics, 2009. *Ca-Cancer J. Clin.* 59, 225–249.
- (2) Oudard, S. (2013) Progress in emerging therapies for advanced prostate cancer. *Cancer Treat. Rev.* 39, 275–289.
- (3) Clegg, N. J., Wongvipat, J., Joseph, J. D., Tran, C., Ouk, S., Dilhas, A., Chen, Y., Grillot, K., Bischoff, E. D., Cai, L., et al. (2012) ARN-509: a novel antiandrogen for prostate cancer treatment. *Cancer Res.* 72, 1494–1503.
- (4) Berthold, D. R., Sternberg, C. N., and Tannock, I. F. (2005) Management of advanced prostate cancer after first-line chemotherapy. *J. Clin. Oncol.* 23, 8247–8252.
- (5) Tannock, I. F., De Wit, R., Berry, W. R., Horti, J., Pluzanska, A., Chi, K. N., Oudard, S., Théodore, C., James, N. D., Turesson, I., et al. (2004) Docetaxel plus prednisone or mitoxantrone plus prednisone for advanced prostate cancer. *N. Engl. J. Med.* 351, 1502–1512.
- (6) Beltran, H., Beer, T. M., Carducci, M. A., De Bono, J., Gleave, M., Hussain, M., Kelly, W. K., Saad, F., Sternberg, C., Tagawa, S. T., et al. (2011) New therapies for castration-resistant prostate cancer: efficacy and safety. *Eur. Urol.* 60, 279–290.

- (7) Mohler, M. L., Coss, C. C., Duke, C. B., Patil, S. A., Miller, D. D., and Dalton, J. T. (2012) Androgen receptor antagonists: a patent review (2008–2011). *Expert Opin. Ther. Pat.* 22, 541–565.
- (8) Balbas, M. D., Evans, M. J., Hosfield, D. J., Wongvipat, J., Arora, V. K., Watson, P. A., Chen, Y., Greene, G. L., Shen, Y., and Sawyers, C. L. (2013) Overcoming mutation-based resistance to antiandrogens with rational drug design. *eLife* 2, e00499.
- (9) Nique, F., Hebbe, S., Peixoto, C., Annoot, D., Lefrançois, J.-M., Duval, E., Michoux, L., Triballeau, N., Lemoullec, J.-M., Mollat, P., et al. (2012) Discovery of diarylhydantoins as new selective androgen receptor modulators. *J. Med. Chem.* 55, 8225–8235.
- (10) Koupparis, A., and Gleave, M. E. (2010) Multimodal approaches to high-risk prostate cancer. *Curr. Oncol.* 17 (Supp. 2), S32–S37.
- (11) Dolmans, D. E. J. G. J., Fukumura, D., and Jain, R. K. (2003) Photodynamic therapy for cancer. *Nat. Rev. Cancer* 3, 380–387.
- (12) Azzouzi, A.-R., Barret, E., Moore, C. M., Villers, A., Allen, C., Scherz, A., Muir, G., De Wildt, M., Barber, N. J., Lebdaï, S., and Emberton, M. (2013) TOOKAD(®) Soluble vascular-targeted photodynamic (VTP) therapy: determination of optimal treatment conditions and assessment of effects in patients with localised prostate cancer. *BJU Int.* 112, 766–774.
- (13) Agostinis, P., Berg, K., Cengel, K. A., Foster, T. H., Girotti, A. W., Gollnick, S. O., Hahn, S. M., Hamblin, M. R., Juzeniene, A., Kessel, D., Korbelik, M., Moan, J., Mroz, P., Nowis, D., Piette, J., Wilson, B. C., and Golab, J. (2011) Photodynamic therapy of cancer: an update. *Cancer J. Clin.* 61, 250–281.
- (14) Yoon, I., Li, J. Z., and Shim, Y. K. (2013) Advance in photosensitizers and light delivery for photodynamic therapy. *Clin. Endosc.* 46, 7–23.
- (15) Kinoyama, I., Taniguchi, N., Toyoshima, A., Nozawa, E., Kamikubo, T., Imamura, M., Matsuhisa, A., Samizu, K., Kawaninami, E., Niimi, T., et al. (2006) (+)-(2R,5S)-4-[4-cyano-3-(trifluoromethyl)phenyl]-2,5-dimethyl-N-[6-(trifluoromethyl)pyridin-3-yl]piperazine-1-carboxamide (YM580) as an orally potent and peripherally selective nonsteroidal androgen receptor antagonist. *J. Med. Chem.* 49, 716–726.
- (16) Dreaden, E. C., Gryder, B. E., Austin, L. A., Tene Defo, B. A., Hayden, S. C., Pi, M., Quarles, L. D., Oyeler, A. K., and El-Sayed, M. A. (2012) Antiandrogen gold nanoparticles dual-target and overcome treatment resistance in hormone-insensitive prostate cancer cells. *Bioconjugate Chem.* 23, 1507–1512.
- (17) Gryder, B. E., Akbashev, M. J., Rood, M. K., Raftery, E. D., Meyers, W. M., Dillard, P., Khan, S., and Oyeler, A. K. (2013) Selectively targeting prostate cancer with antiandrogen equipped histone deacetylase inhibitors. *ACS Chem. Biol.* 8, 2550–2560.
- (18) Carpenter, A. W., and Schoenfish, M. H. (2012) Nitric oxide release: part II. Therapeutic applications. *Chem. Soc. Rev.* 41, 3742–3752.
- (19) Jenkins, C. D., Charles, I. G., Thomsen, L. L., Moss, D. W., Holmes, L. S., Baylis, S. A., Rhodes, P., Westmore, K., Emson, P. C., and Moncada, S. (1995) Role of nitric oxide in tumor growth. *Proc. Natl. Acad. Sci. U. S. A.* 92, 4392–4396.
- (20) Gupta, S., Ahmad, N., and Mukhtar, H. (1998) Involvement of nitric oxide during phthalocyanine (Pc4) photodynamic therapy-mediated apoptosis. *Cancer Res.* 58, 1785–1788.
- (21) Korbelik, M., Parkins, C. S., Shibuya, H., Cecic, I., Stratford, M. R., and Chaplin, D. J. (2000) Nitric oxide production by tumour tissue: impact on the response to photodynamic therapy. *Br. J. Cancer* 82, 1835–1843.
- (22) Rapozzi, V., Della Pietra, E., Zorzet, S., Zacchigna, M., Bonavida, B., and Xodo, L. E. (2013) Nitric oxide-mediated activity in anti-cancer photodynamic therapy. *Nitric Oxide* 30, 26–35.
- (23) Carneiro, Z. A., De Moraes, J. C. B., Rodrigues, F. P., De Lima, R. G., Curti, C., Da Rocha, Z. N., Paulo, M., Bendhack, L. M., Tedesco, A. C., Formiga, A. L. B., and Da Silva, R. S. (2011) Photocytotoxic activity of a nitrosyl phthalocyanine ruthenium complex - A system capable of producing nitric oxide and singlet oxygen. *J. Inorg. Biochem.* 105, 1035–1043.
- (24) Kim, J., Saravanakumar, G., Choi, H. W., Park, D., and Kim, W. J. (2014) A platform for nitric oxide delivery. *J. Mater. Chem. B* 2, 341–356.
- (25) Sortino, S. (2010) Light-controlled nitric oxide delivering molecular assemblies. *Chem. Soc. Rev.* 39, 2903–2913.
- (26) Nobuaki, T., Isao, K., Takashi, K., Akira, T., Kiyohiro, S., Eiji, K., Masakazu, I., Hiroyuki, M., Akira, M., Masaaki, H., et al. (2004) Cyanophenyl derivative Patent Number WO/2000/017163.
- (27) Migliaccio, A., Castoria, G., Di Domenico, M., De Falco, A., Bilancio, A., Lombardi, M., Barone, M. V., Ametrano, D., Zannini, M. S., Abbondanza, C., et al. (2000) Steroid-induced androgen receptor-oestradiol receptor beta-Src complex triggers prostate cancer cell proliferation. *EMBO J.* 19, 5406–5417.
- (28) Castoria, G., Giovannelli, P., Di Donato, M., Ciociola, A., Hayashi, R., Bernal, F., Appella, E., Auricchio, F., and Migliaccio, A. (2014) Role of non-genomic androgen signalling in suppressing proliferation of fibroblasts and fibrosarcoma cells. *Cell Death Dis.* 5, e1548.
- (29) Tomlins, S. A., Rhodes, D. R., Perner, S., Dhanasekaran, S. M., Mehra, R., Sun, X.-W., Varambally, S., Cao, X., Tchinda, J., Kuefer, R., et al. (2005) Recurrent fusion of TMPRSS2 and ETS transcription factor genes in prostate cancer. *Science* 310, 644–648.
- (30) Tai, S., Sun, Y., Squires, J. M., Zhang, H., Oh, W. K., Liang, C.-Z., and Huang, J. (2011) PC3 is a cell line characteristic of prostatic small cell carcinoma. *Prostate* 71, 1668–1679.
- (31) Alimirah, F., Chen, J., Basrawala, Z., Xin, H., and Choubey, D. (2006) DU-145 and PC-3 human prostate cancer cell lines express androgen receptor: Implications for the androgen receptor functions and regulation. *FEBS Lett.* 580, 2294–2300.
- (32) Rapozzi, V., and Jori, G. (2015) Resistance to Targeted Anti-Cancer Therapeutics. In *Resistance to Photodynamic Therapy in Cancer Vol. 5* (Rapozzi, V., and Jori, G., Eds.) pp 3–26, Chapter 1, Springer Press.
- (33) Robey, R. W., Steadman, K., Polgar, O., Morisaki, K., Blayney, M., Mistry, P., and Bates, S. E. (2004) Pheophorbide a is a specific probe for ABCG2 function and inhibition. *Cancer Res.* 64, 1242–1246.
- (34) Robey, R. W., Steadman, K., Polgar, O., and Bates, S. E. (2005) ABCG2-mediated transport of photosensitizers: Potential impact on photodynamic therapy. *Cancer Biol. Ther.* 4, 187–194.
- (35) Selbo, P. K., Weyergang, A., Eng, M. S., Bostad, M., Mælandsmo, G. M., Hogset, A., and Berg, K. (2012) Strongly amphiphilic photosensitizers are not substrates of the cancer stem cell marker ABCG2 and provides specific and efficient light-triggered drug delivery of an EGFR-targeted cytotoxic drug. *J. Controlled Release* 159, 197–203.
- (36) Ingram, W. J., Crowther, L. M., Little, E. B., Freeman, R., Harliwong, I., Veleza, D., Hassall, T. E., Remke, M., Taylor, M. D., and Hallahan, A. R. (2013) ABC transporter activity linked to radiation resistance and molecular subtype in pediatric medulloblastoma. *Exp. Hematol. Oncol.* 2, 26–43.
- (37) Bessho, Y., Oguri, T., Achiwa, H., Muramatsu, H., Maeda, H., Niimi, T., Sato, S., and Ueda, R. (2006) Role of ABCG2 as a biomarker for predicting resistance to CPT-11/SN-38 in lung cancer. *Cancer Sci.* 97, 192–198.
- (38) Castoria, G., D'Amato, L., Ciociola, A., Giovannelli, P., Giraldi, T., Sepe, L., Paoletta, G., Barone, M. V., Migliaccio, A., and Auricchio, F. (2011) Androgen-induced cell migration: role of androgen receptor/filamin A association. *PLoS One* 6, e17218.
- (39) Tesei, A., Leonetti, C., Di Donato, M., Gabucci, E., Porru, M., Varchi, G., Guerrini, A., Amadori, D., Arienti, C., Pignatta, S., et al. (2013) Effect of Small Molecules Modulating Androgen Receptor (SARMs) in Human Prostate Cancer Models. *PLoS One* 8, e62657.